frontiers in Materials

ORIGINAL RESEARCH
published: 08 March 2022
doi: 10.3389/fmats.2022.811838

Effect of Material Composition on Freeze-Thaw Resistance of Asphalt Fine Aggregate Matrix at Low-Temperatures From Mesoscopic Perspective

Xiangbing Gong[1,2]*, *Heqi Zheng*[2], *Wei Liu*[2] *and Xi Li*[2]

[1]State Engineering Laboratory of Highway Maintenance Technology, Changsha University of Science and Technology, Changsha, China, [2]School of Traffic and Transportation Engineering, Changsha University of Science and Technology, Changsha, China

To explore the significant factors related to the cracking resistance at low temperatures of asphalt mixture from mesoscopic perspective, asphalt fine aggregate matrix (FAM) was selected as the researched material because of its important role in mesoscopic structure of asphalt mixture. Bending Beam Rheometer (BBR) was utilized to investigate low-temperature properties of FAM. Due to the frequent occurrence of freeze-thaw action in seasonally frozen regions, this paper introduces a freeze-thaw cycle test. The structural characteristics of internal air voids in FAM and hot-mix asphalt (HMA) were analyzed using the industrial Computerized Tomography (CT). Results indicate that frost heaving damage of FAM-2.36 is more obvious than that of FAM-1.18, and the damage level increases as the bath temperature rises. After 32 freeze-thaw cycles, FAM-1.18 exhibits the rise of creep stiffness than original beams, and the hardening degree become serious with the decease of temperature. It could be concluded that the BBR has been proved to be an effective tool in evaluating the low-temperature properties of FAM. The expanding limit of small air voids and the hardening of binder in rich asphalt FAM contribute to completely different mechanisms of freezing-thawing damage within FAM. Therefore, asphalt content, fine aggregate passing rate and air voids size could be optimized through BBR test of FAM subjected to freeze-thaw cycle.

Keywords: freeze-thaw cycle, bending beam rheometer, asphalt fine aggregate matrix, low-temperature property, mesoscale, frost heave, hardening

OPEN ACCESS

Edited by:
Goshtasp Cheraghian, Technische Universitat Braunschweig, Germany

Reviewed by:
Shengfu Wang, East China University of Technology, China
Figen Balo, Firat University, Turkey

***Correspondence:**
Xiangbing Gong
xbgong@csust.edu.cn

Specialty section:
This article was submitted to Structural Materials, a section of the journal Frontiers in Materials

Received: *09 November 2021*
Accepted: *22 February 2022*
Published: *08 March 2022*

Citation:
Gong X, Zheng H, Liu W and Li X (2022) Effect of Material Composition on Freeze-Thaw Resistance of Asphalt Fine Aggregate Matrix at Low-Temperatures From Mesoscopic Perspective. Front. Mater. 9:811838. doi: 10.3389/fmats.2022.811838

1 INTRODUCTION

Asphalt pavements are commonly used in highway pavement projects (Qian et al., 2021). However, in seasonal freezing areas, freeze-thaw damage frequently occurs due to the large range of temperature changes between day and night, causing damage to the asphalt mixture such as loosening, falling particles, and potholes, reducing the overall strength and service life of the asphalt pavement (Wang et al., 2013; Shan et al., 2020; Li et al., 2021). Therefore, freeze-thaw cycle experiments has been used to simulate natural conditions of asphalt mixture for decades and evaluate

the resistance to freeze-thaw damage (Xu et al., 2016; Karimi et al., 2021). However, Xu et al. (2015) found that the internal structure at mesoscale was sensitive to the freeze-thaw action and ignored in current material design method of asphalt mixture.

Current researchers suggest that an asphalt mixture can be seen as a non-homogeneous multi-phase composite consisting of asphalt fine aggregate matrix (FAM), coarse aggregates, and voids at mesoscale (Wang et al., 2020; Han et al., 2021). Although the proportion of FAM in the mixture is relatively small, the FAM provides the necessary strength (Chuanfeng et al., 2017), fills the skeletal voids, provides internal bonding between the skeletons (Qian et al., 2016; Xing et al., 2021; Zhang et al., 2021), and known as a component in influencing the performance of the mixture (Shi et al., 2020). Therefore, the mechanical properties of FAM under different environmental conditions should be included to furtherly understand the mechanical properties of asphalt mixtures. Du et al. (2021) analyzed the influence of aggregates of different particle sizes on the anti-cracking effect of FAM at low temperatures. Yu et al. (2021) tested the influence of UV ageing time and strength on styrene-butadiene-styrene (SBS) modified FAM and found that the flexural modulus of the FAM increased with rising of UV intensity and ageing time. Zhang and Leng (2017) studied the effect of basalt fiber on the crack resistance of FAM. The results showed that adding a proper amount of basalt fiber could effectively improve the mechanical properties of FAM. Cui et al. (2017) studied the structural changes of FAM during freeze-thaw cycles at different salt concentrations through uniaxial creep tests and scanning electron microscopy (SEM). FAM plays an important role in maintaining the performance of asphalt mixture especially for the low-temperature cracking (Dong et al., 2014), it is significant to conduct comprehensive testing on FAM and consider the influence of freeze-thaw cycle.

Current research methods of FAM always are derived from the research methods of asphalt mixture. Although Indirect Tensile test (IDT) (Amin and Esmail, 2017), Semi-Circular Bending test (SCB) (Ameri et al., 2012; Yang et al., 2021), Dynamic Shear Rheometer (DSR) (Zhou et al., 2019), Thermal Stress Restrained Specimen Test (TSRST) (Keshavarzi et al., 2021) have been used in related studies to evaluate the low-temperature performance of FAM. However, the preparation of specimens, experimental procedures and data collection are quite complex for the tests mentioned above. Therefore, scholars have proposed the use of a simple Bending Beam Rheometer (BBR) test to evaluate the low-temperature performance of FAM (Marasteanu et al., 2016; Gong et al., 2017). The BBR test is usually used to capture the creep stiffness (*S*) and relaxation rate (*m* value) of FAM in the beam geometry, and it can evaluate the low-temperature performance of both asphalt and asphalt mixture (Moon et al., 2013; Wang et al., 2022). To verify the influence of the size of the BBR beam, Velásquez et al. (2009) compared the creep stiffness curves of different sizes of mixed beams (1 time, 2 times, and 3 times the size of the BBR beam) and concluded that when the test temperature is 10°C higher than the lowest limit of the PG classification, the influence of size on creep stiffness can be overlooked. Moreover, Romero and Weissan (Weissman et al., 1999; Romero and Masad, 2001) discussed the influence of specimen size on the test results based on the Representative Volume Element method (RVE), and they concluded that the thin beam meets the minimum RVE requirement. It can be seen that the size of BBR can meet the requirements of the low-temperature performance test of asphalt FAM according the reproducibility of FAM BBR tests (Yin et al., 2011; Gong et al., 2016). Nevertheless, FAM is well known as a complex multi-scale, multi-layer, and multi-component material (Underwood and Kim, 2013), fine aggregate size, asphalt content, and air voids are typical factors to be directly related to the low-temperature performance of FAM in extremely cold regions.

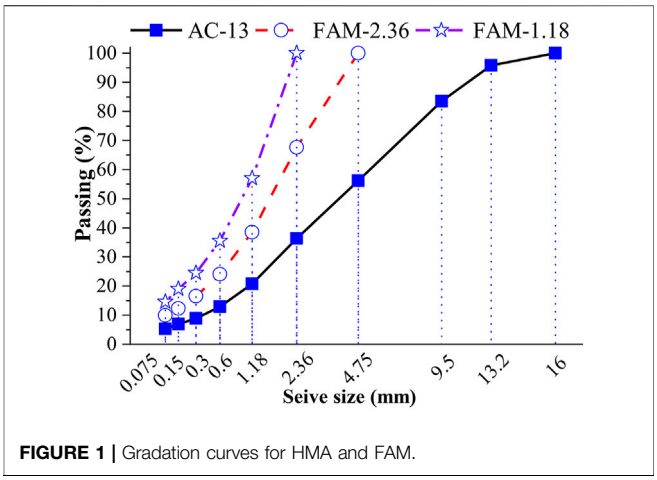

FIGURE 1 | Gradation curves for HMA and FAM.

The effect of freeze-thaw cycle on asphalt pavement in seasonal frozen regions should include the performance evaluation of FAM at mesoscale not merely using macroscopic evaluation indexes. Therefore, this paper applies BBR to evaluating the low-temperature performance of FAM subjected to different freeze-thaw cycles, and explores the main factors leading to low-temperature shrinkage cracking in asphalt pavements at mesoscale. Furthermore, different FAMs, different temperatures, and different cycles were set up in the test to including the factors. Industrial Computerized Tomography (CT) was used to extract the mesoscopic air voids. Finally, this study explored the effect of asphalt content and the air void structure on the freeze-thaw damage of the FAM associated with the resistance to the thermal cracking of FAM.

2 CALCULATION OF ASPHALT CONTENT IN FAM

The FAM in the asphalt mixture consists of fine aggregate, asphalt adsorbed by the fine aggregate, effective asphalt, and voids. The ratio of the fine aggregate content of each grade in the FAM grading scheme is consistent with the proportion in the asphalt mixture, thereby yielding the passing rate of the fine aggregate of the FAM. To investigate the effect of fine aggregate ratio and asphalt content on its low-temperature performance of FAM, the equivalent FAM-2.36 (maximum particle size 2.36 mm) and

TABLE 1 | Volumetric parameters of FAM.

FAM	P_{ba}	P_i	FB	P'_b	a'_f
FAM-2.36	0.20	56.2	1.30	7.15	9.9
FAM-1.18		36.3		10.15	14.6

FAM-1.18 (maximum particle size 1.18 mm) gradation curve was calculated based on the same AC-13 (aggregates with nominal maximum particle size of 13 mm) mixture gradation. All gradation curves of asphalt mixture and FAMs are shown in **Figure 1**. According to the Superpave mixture volume index design method, the optimum asphalt content of AC-13 was determined to be 4.10% (P_b), the corresponding air void ratio was 3.9%, and the number of rotary compaction was 70 times. The calculation of the equivalent asphalt content in the FAM is as follows. The asphalt which not absorbed by the aggregate in the asphalt mixture is called effective asphalt. The ratio of the pass rate of the 0.075 mm mesh hole to the effective asphalt content in the mixed mineral material is called the ratio of filler bitumen. Based on the calculation method of the ratio of filler bitumen (Gong et al., 2017), according to the principle that the FAM and asphalt mixture has the same ratio of filler bitumen, the calculation method of fine aggregate matrix and asphalt content is derived. Based on the parameter values provided in **Table 1**, the asphalt content of the FAM was calculated.

Table Note: P'_b is the asphalt content (%) in FAM; a'_f is the mineral powder content (%) in FAM; P_{ba} is the asphalt binder absorbed by aggregate in asphalt mixture Proportion (%); P_i is the pass rate of the key mesh of the fine aggregate in the asphalt mixture. I take 4.75 and 2.36 (%) respectively; *FB* is the ratio of filler bitumen of the asphalt mixture.

FIGURE 2 | CT images of FAM and HMA beams.

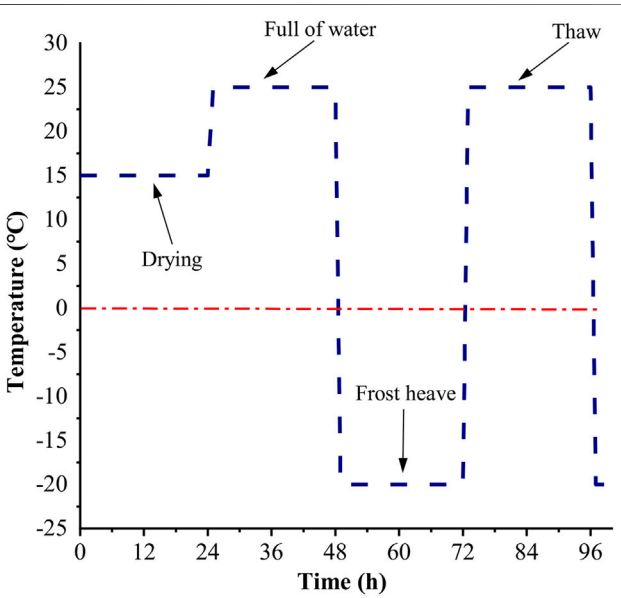

FIGURE 3 | Depiction of the first freeze–thaw cycle.

3 SAMPLE PREPARATION AND TEST METHODS

3.1 Preparation of FAM BBR Beam

The BBR beam was cut from the test piece of FAM formed by the laboratory. The corresponding preparation process included preparation of cylindrical FAM specimens and cutting of FAM BBR beams. FAM cylindrical specimens are usually isostatic pressing (Fadil et al., 2019; Fonseca et al., 2019) and gyratory (Dong et al., 2014). To accurately simulate the role of the roller in the construction process of asphalt pavement, this paper has selected the gyratory compactor to form a cylindrical test piece (Φ150×h100 mm). Since the FAM samples remove the coarse aggregate skeleton from Hot-mix Asphalt (HMA) the number of rotations has been reduced from 70 times of HMA (AC-13) to 50 times of FAM. The binder PG used in the FAM was classified into PG 64-28. Since the asphalt content in the FAM is high and the mineral materials are fine aggregates, the blending duration was increased to 5 min.

The cutting process of the BBR beams of FAM is described as follows. After the specimen is left to cooling for 24 h, the position of the inscribed rectangular parallelepiped of the cylindrical specimen was marked; the cylinder was cut into a rectangular body by a large cutting machine, and the rectangular parallelepiped was divided into two. The long square test piece was sequentially fixed on the small cutting machine, and after cutting off the top and the end of the test piece with a large void ratio, it was cut into strips of width 12.5 ± 0.25 mm. The strip was modelled into a FAM beam of thickness of 6.25 ± 0.25 mm and a length of 127 ± 0.25 mm. The BBR beam pictures are listed in **Figure 2**, they are FAM-2.36, FAM-1.18, and AC-13 from left to right. For the BBR test of FAM and HMA, testing method increase the creep load to 4,400 ± 100 mN (Ho and Romero, 2011), and the rest of the operation is consistent with the asphalt binder BBR test specification. After the beams were soaked for 60 ± 2 min in a constant temperature bath, they were placed in the specimen holder, and the creep load was applied for 240s. The deformation values were recorded and the creep stiffness and *m* value were calculated.

3.2 Freeze-Thaw Cycle

Four freeze-thaw cycles (4 times, 8 times, 16 times, 32 times) and three temperatures (−18°C, −12°C, −6°C) were set as BBR test variables. The freeze-thaw cycle test procedure of the FAM BBR beam is presented as follows (Gong et al., 2017). First, the dry

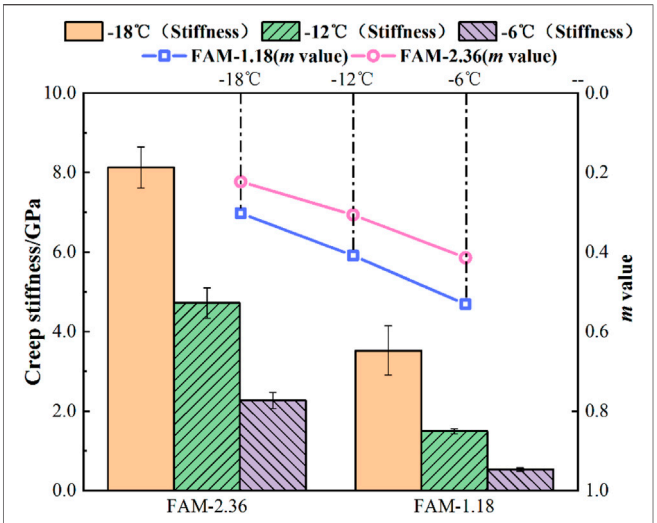

FIGURE 4 | Creep stiffness and *m* value at 60 s for original FAM at various low temperatures.

weight of the FAM beam was naturally dried after being dried at room temperature. Next, the FAM beam was immersed in a constant temperature water bath at a temperature of 25 ± 0.25°C for 24 h. Then, the FAM beam was lifted out from the water bath and wiped to reach the saturated surface dry (SSD) condition. After the SSD weight contending water in the inner air voids of beams was weighed, the BBR beam was placed in an air bath at a temperature of −20 ± 0.25°C for 24 h. Finally, the BBR beam in the air bath was taken out and immersed in a constant temperature water bath of 25 ± 0.25°C for 24 h to complete a freeze-thaw cycle. The relevant description is illustrated in **Figure 3**. The sample volume of each test control group was five. The original FAM, which had not undergone any freeze-thaw cycle, was set as the reference group. All masses were weighed to the nearest 0.01 g for the calculation of the water absorption of the FAM using dry weight and SSD weight. To ensure the reliability of the test data, the coefficient of variation of all test results must all have met the requirements of being less than 10%.

4 ANALYSIS OF TEST RESULT

4.1 Evaluation of the Low-Temperature Performance of Original FAM

Consistent with the asphalt binder BBR test specification, the creep stiffness and *m* value at 60s were used to evaluate the low-temperature performance of the original FAM, as depicted in **Figure 4**. It can be inferred that the error value of each test group increases with the decrease of test temperature, but both meet the requirement of coefficient of variation of being less than 10%.Therefore, the BBR test is proved to be a stable and effective method for evaluating the low-temperature performance of FAM. With the increase of the test temperature, the creep stiffness at 60s shows a decreasing with the equal proportion, and the decreasing ratio is approximate 2. Moreover, the *m* value at 60s shows a linear increasing law with increasing amplitude of about 0.1. Along the change of test temperature, the BBR evaluation method showed that the low-temperature shrinkage stress of FAM-1.18 was lower than that of FAM-2.36, and the relaxation ability exceeded that of FAM-2.36. It can be seen that the low temperature cracking rate of FAM-1.18 is less than FAM-2.36. Based on the above analysis, the proportion of fine aggregate in the asphalt mixture gradation and the asphalt content is significantly linked to the resistance to low temperature cracking ability of FAM.

4.2 Water Absorption Rate

This paper used the water absorption rate to indirectly reflect the severity of freeze-thaw damage (Feng et al., 2010; Cui et al., 2017). The change of water absorption rate of FAM with the number of freeze-thaw cycles at 25 ± 0.25°C is illustrated in **Figure 5**. The water absorption rate of FAM was directly related to the number of freeze-thaw cycles. The more number of freeze-thaw cycles increased between two adjacent controlling groups, and the more obvious increase of water absorption rate, as shown by the histograms of 16 and 32 times. In the initial stage of the freeze-thaw cycle, the water absorption of FAM-2.36 and FAM-1.18 does not possess significant differences. However, when the number of freeze-thaw cycles increased to 32, the water absorption was significantly different, and the difference between FAM-2,36 and FAM-1.18 increased from 0.003% at four cycles to 0.059% at32 cycles. Based on this analysis, FAM-2.36 has been found to be more sensitive to the freeze-thaw cycle than FAM-1.18, and the frost heaving force causes more serious frost heaving damage inside FAM-2.36. It can also be implied that the proportion of fine aggregates in the asphalt mixture and the amount of asphalt binder will directly affect the ability of the FAM to resist frost heave damage at mesoscale.

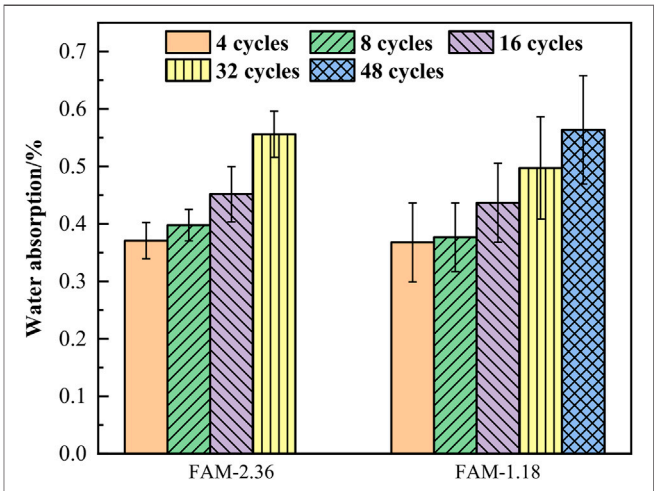

FIGURE 5 | Water absorption of FAM subjected to different freeze-thaw cycles.

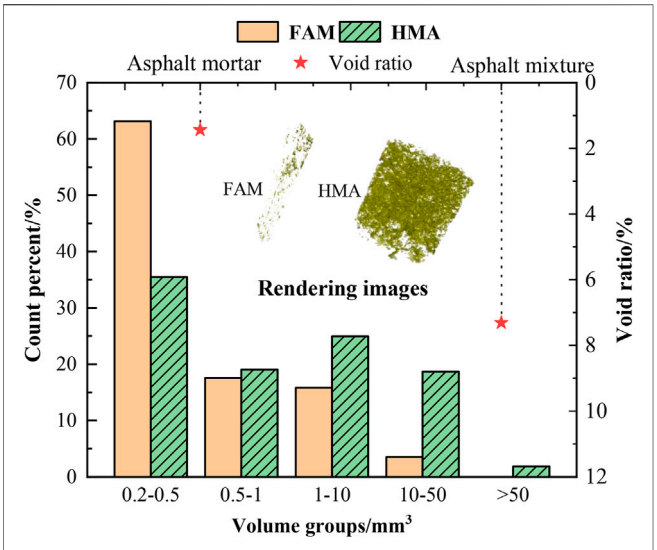

FIGURE 6 | Volume distribution of air voids and the air void content.

4.3 Evaluation on Freeze-Thaw Resistance of FAM

4.3.1 Analysis of Air Voids Based on CT

In this paper, industrial CT was used to study the difference of the void structure characteristics between FAM and HMA, and the three-dimensional digital reconstruction and data analysis of the internal voids of the material was finally completed. **Figure 6** depicts that the air void content of the asphalt mixture (7.31%) is about five times that of the FAM (1.44%). Moreover, the three-dimensional rendering images of the voids shows that the average void size of HMA is remarkably different from that of the FAM. The volume of the voids was extracted and calculated based on the voxel analysis software (VGStudio Max 2.2) and divided into five groups. **Figure 6** illustrates that the small voids (0.2–0.1 mm^3) of the FAM with a cumulative percentage exceeding 75% and no large pores (>50 mm^3). Furthermore, the proportion of voids in the FAM shows a stepwise decreasing trend with the void volume increase. Relatively speaking, the proportion of small voids (0.2–1 mm^3) and intermediate voids (1–50 mm^3) in HMA is balanced, and there is a certain proportion of large holes. It was concluded that a large number of small voids in the FAM is a crucial factor to resisting the freeze-thaw cycles, and more independent and small voids in FAM will cause more serious freeze-thaw damage due to the expanding volume limit.

4.3.2 Analysis of Test Results of FAM-2.36

The original FAM was used as the reference group in this study to calculate the changing percent of testing variables. The 60s creep stiffness and the percentage change of *m* value were used as the evaluation indexes, wherein the positive value indicates decreasing and the negative value indicates an increase. The creep stiffness of FAM-2.36 in **Figure 7** depicts a certain decreasing trend with the number of freeze-thaw cycles increasing. This phenomenon is similar to the increase of water absorption rate with the number of freeze-thaw cycles. Therefore, the reduction in the creep stiffness of FAM-2.36 has a certain correlation with the frost-heaving damage in small voids. Furthermore, the damage of the FAM-2.36 gets more serious with the rising of testing temperature, which is associated with that freeze-thaw damage of the actual asphalt pavement mainly occurs in the early spring.

In this paper, AC-13 and FAM-2.36 were established to explore the influence of air void structure on freeze-thaw damage. The material parameters are listed in **Table 2**, wherein HMA and FAM represent AC-13 and FAM-2.36. Based on the principle of controlling asphalt content the same and changing the number of compaction, the preparation of BBR beams with different air void content was finished. The calculation of the asphalt content in FAM-2.36 and the determination of the number of compaction based on the method mentioned above. The results of material parameters of reference groups at −18°C and 60s are listed in **Table 2**. Regarding the influence trend due to air void content, FAM-2.36 showed an opposite effect contrasting to HMA (AC-13), as results illustrated in **Figure 8**. After four freeze-thaw cycles, the decreased rate of creep stiffness of HMA-1 and FAM-2 keep at a higher rate. After 32 freeze-thaw cycles, the decreased rate of creep stiffness of HMA-2 and FAM-1 beyond the former one. The results show that under the condition of the long-term freeze-thaw cycle, the macroscopic connected air voids in HMA can help mitigate the erosion of the frost-heaving force in the air void saturated with water. However, the small air void in FAM is similar to the frost heave mechanism of the microscopic pores in cement material (Eskişar et al., 2015; Fan et al., 2020), and the water cannot be easily drained so that the frost-heave force of the saturated water air void cannot be promptly dissipated.

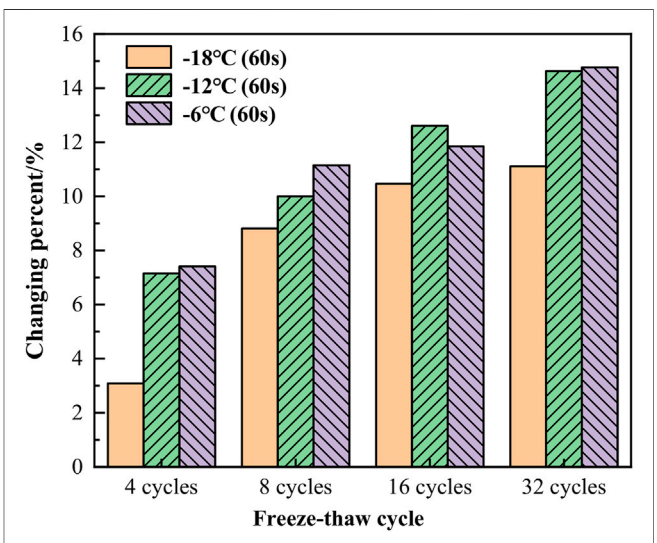

FIGURE 7 | Changing percent of creep stiffness for FAM-2.36 subjected to different free-thaw cycles.

TABLE 2 | Material parameters and virgin BBR testing results of HMA and FAM.

BBR beams	Compaction number	Asphalt content (%)	Stiffness (GPa, 60s)	*m* value (60s)
HMA-1 (AC-13)	50	4.15	15.4	0.134
HMA-2 (AC-13)	70		18.2	0.129
FAM-1 (FAM-2.36)	30	6.92	8.6	0.194
FAM-2 (FAM-2.36)	50		9.5	0.182

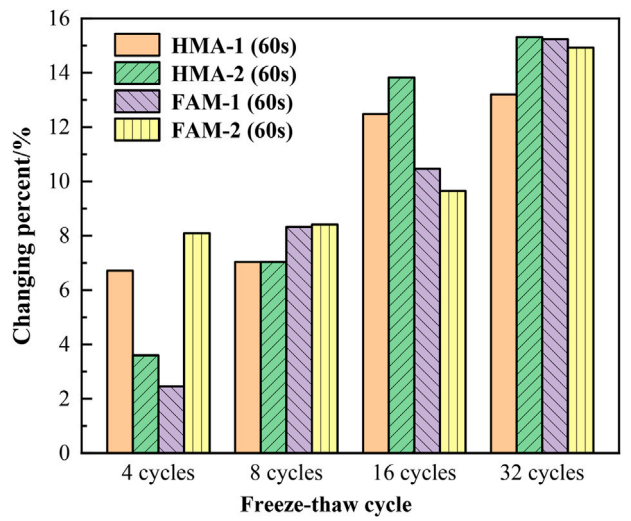

FIGURE 8 | Changing percent of creep stiffness forFAM-2.36 and AC-13 BBR beams with various air void contents (−18°C).

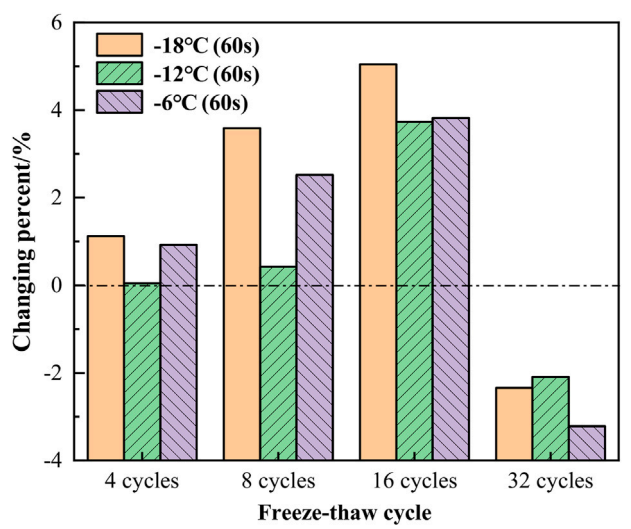

FIGURE 9 | Changing percent of creep stiffness at 60s for FAM-1.18 subjected to different freeze-thaw cycles.

4.3.3 Analysis of Test Results of FAM-1.18

Different from the freeze-thaw damage mechanism exhibited by FAM-2.36, the creep stiffness of FAM-1.18 appears to decrease

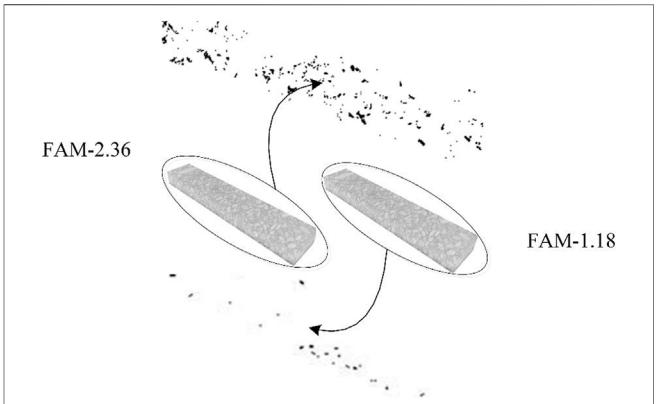

FIGURE 10 | Air voids industrial CT rendering images of FAM-2.36 and FAM-1.18.

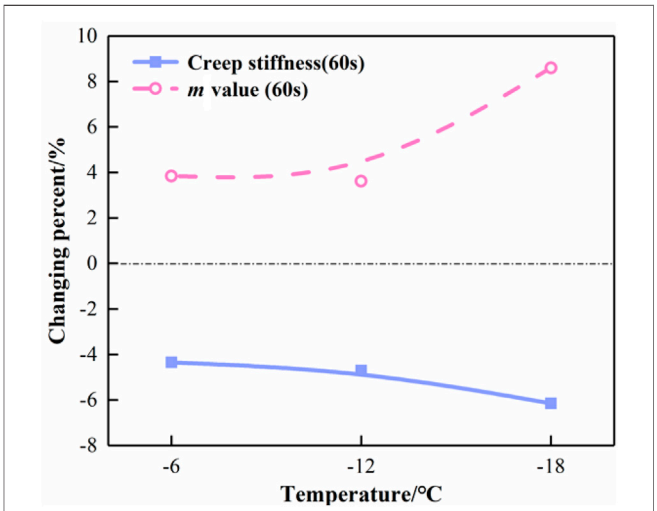

FIGURE 11 | Changing percent of creep stiffness and *m* value of FAM-1.18 at different temperatures and 48 Cycles.

first and then increase, and the turning point appears at 32 freeze-thaw cycles, as shown in **Figure 9**. The maximum creep stiffness reduction rate for FAM-1.18 occurs at −18°C, but for FAM-2.36 occurs at −6°C. In the early freezing and thawing cycle, the frost heaving force in the small air void of FAM-1.18 due to saturated water is still the dominant factor of its freeze-thaw damage. However, the increase in water absorption rate indicates that the degree of freeze-thaw damage of FAM-1.18 did not increase significantly when compared to FAM-2.36, which can be

TABLE 3 | Changing percent of *m* value for FAM-1.18 at different temperatures and cycles.

Indexes	Cycle	−18°C	−12°C	−6°C
m value	32	3.025	1.026	2.712
	48	8.597	3.618	3.843

explained by the small air void amount difference between FAM-1.18 and FAM-2.36 shown in **Figure 10**. It can be seen that the high content of asphalt in FAM-1.18 can enhance the frost heaving damage of FAM to a certain extent. Furthermore, the creep stiffness of FAM-1.18 increases after a long period of water-saturated melting comparing to the origin beams in **Figure 4**. It can be assumed that water soaked hardening of asphalt binder become the dominant factor, which is related to the high asphalt content FAM-1.18.

To further verify the existence of water soaked hardening, the number of freeze-thaw cycle of FAM-1.18 was increased to 48 times. The increase of water absorption in **Figure 5** at 48 cycles indicates that the competitive relationship between water soaked hardening and frost-heaving damage in FAM-1.18 has been reversed. **Figure 11** presents that creep stiffness of FAM-1.18 increases and the *m* value of FAM-1.18 decreases along the freeze-thaw cycle increases from 32 times to 48 times shown in **Figure 9** and **Table 3**. This trend indicates that the shrinkage stress of FAM-1.18 increases and relaxation ability is weakened subjected to long-term freeze-thaw cycles: Therefore, water soaked hardening increases the low-temperature cracking rate of FAM-1.18. The maximum changing percent in creep stiffness and *m* value occurs at -18°C. It was found that the water soaked hardening caused by long-term freeze-thaw cycle is obviously dependent on the temperature and significantly degrades the resistance to cracking of FMA-1.18 especially in extremely cold regions. The hardening found above could be related to the former studies named as the water-saturated emulsification mechanism (Camacho-Garita et al., 2019) and the water-saturated aging mechanism (Thomas, 2002; Yu et al., 2020). However, accurate water soaked hardening mechanisms of finer FAM still require extensive research. In summary, the asphalt content, fine aggregate ratio and air void difference of are critical factors, which affects the damage mechanism of FAM undergoing a long-term freeze-thaw cycle in asphalt pavements at mesoscale.

5 CONCLUSION

1) The coefficient of variation results shows that the BBR is suitable to conduct the low-temperature performance evaluation of FAM. The comparative analysis of creep stiffness and *m* value of FAM at 60s including the freeze-thaw cycle could be used to determine the best the asphalt content, fine aggregate passing rate, and air void structure in asphalt mixture material design.
2) Similar to the frost-heaving mechanism of microscopic air voids in cement materials, the small air voids in FAM are the main cause of frost-heaving damage due to the expansion limit of freezing water. However, the asphalt content and fine aggregate content in FAM determines its ability to resist the frost heaving damage.
3) Rich asphalt content in FAM brings higher low-temperature cracking rate of asphalt pavements subjected to long-term freeze-thaw cycle especially at extremely cold regions, the water soaked hardening mechanism of FAM could be explained by the emulsification and aging of asphalt binder reacted with the water for a long duration.

DATA AVAILABILITY STATEMENT

The original contributions presented in the study are included in the article/Supplementary Material, further inquiries can be directed to the corresponding author.

AUTHOR CONTRIBUTIONS

XG provided ideas and supervised the experiments. HZ and WL conducted experiments and data analysis. XG and XL directed manuscript writing and checking. HZ and WL completed the figures and tables in the manuscript. All authors have read and agreed to the published version of the manuscript.

FUNDING

The study was supported by the National Natural Science Foundation of China (Grant No.: 51808058, 52078065, and 52078064) and by the Open Fund of State Engineering Laboratory of Highway Maintenance Technology (Changsha University of Science and Technology) (grant No.: kfj170102).

ACKNOWLEDGMENTS

This study was completed at the School of Traffic and Transportation Engineering, in Changsha University of Science and Technology, and School of Transportation Science and Engineering in Harbin Institute of Technology.

REFERENCES

Ameri, M., Mansourian, A., Pirmohammad, S., Aliha, M. R. M., and Ayatollahi, M. R. (2012). Mixed Mode Fracture Resistance of Asphalt concrete Mixtures. *Eng. Fracture Mech.* 93, 153–167. doi:10.1016/j.engfracmech.2012.06.015

Amin, G. M., and Esmail, A. (2017). Application of Nano Silica to Improve Self-Healing of Asphalt Mixes. *J. Cent. South. Univ.* 24, 1019–1026. doi:10.1007/s11771-017-3504-y

Camacho-Garita, E., Aguiar-Moya, J. P., Ávila-Esquivel, T., and Loría-Salazar, L. G. (2019). Effect of Moisture on Full-Scale Pavement Distress. *J. Test. Eval.* 48, 20180902–20181246. doi:10.1520/JTE20180902

Chuanfeng, Z., Yupeng, F., Zhuang, M., and Xue, Y. (2017). Influence of mineral Filler on the Low-Temperature Cohesive Strength of Asphalt Mortar. *Cold Regions Sci. Techn.* 133, 1–6. doi:10.1016/j.coldregions.2016.10.006

Cui, Y., Chen, D. S., Feng, L., and Wang, L. (2017). Effects of Salt Freeze Damage on the Viscoelastic Performance of Asphalt Mortar. *Ceram. Silik.* 3, 257–266. doi:10.13168/cs.2017.0024

Dong, Z., Gong, X., Zhao, L., and Zhang, L. (2014). Mesostructural Damage Simulation of Asphalt Mixture Using Microscopic Interface Contact Models. *Constr. Build. Mater.* 53, 665–673. doi:10.1016/j.conbuildmat.2013.11.109

Du, J., Rahman, A., Zhou, Z., Ai, C., and Qiu, Y. (2021). Enhancement Effect of the Aggregate Particles on the Low-Temperature Cracking Resistance of the Asphalt Mortar. *Constr. Build. Mater.* 290, 123225. doi:10.1016/j.conbuildmat.2021.123225

Eskişar, T., Altun, S., and Kalıpcılar, İ. (2015). Assessment of Strength Development and Freeze-Thaw Performance of Cement Treated Clays at Different Water Contents. *Cold Regions Sci. Techn.* 111, 50–59. doi:10.1016/j.coldregions.2014.12.008

Fadil, H., Jelagin, D., Larsson, P.-L., and Partl, M. N. (2019). Measurement of the Viscoelastic Properties of Asphalt Mortar and its Components with Indentation Tests. *Road Mater. Pavement Des.* 20, S797–S811. doi:10.1080/14680629.2019.1628434

Fan, Z. P., Xu, H. N., Xiao, J. Z., and Tan, Y. Q. (2020). Effects of Freeze-Thaw Cycles on Fatigue Performance of Asphalt Mixture and Development of Fatigue-Freeze-Thaw (FFT) Uniform Equation. *Constr. Build. Mater.* 242, 118043. doi:10.1016/j.conbuildmat.2020.118043

Feng, D., Yi, J., Wang, D., and Chen, L. (2010). Impact of Salt and Freeze-Thaw Cycles on Performance of Asphalt Mixtures in Coastal Frozen Region of China. *Cold Regions Sci. Techn.* 62, 34–41. doi:10.1016/j.coldregions.2010.02.002

Fonseca, J. F., Sudo Lutif Teixeira, J. E., Castelo Branco, V. T. F., and Kim, Y.-R. (2019). Evaluation of Effects of Filler By-Products on fine Aggregate Matrix Viscoelasticity and Fatigue-Fracture Characteristics. *J. Mater. Civ. Eng.* 31, 04019240. doi:10.1061/(asce)mt.1943-5533.0002891

Gong, X., Romero, P., Dong, Z., and Sudbury, D. S. (2016). The Effect of Freeze-Thaw Cycle on the Low-Temperature Properties of Asphalt fine Aggregate Matrix Utilizing Bending Beam Rheometer. *Cold Regions Sci. Techn.* 125, 101–107. doi:10.1016/j.coldregions.2016.02.008

Gong, X., Romero, P., Dong, Z., and Li, Y. (2017). Investigation on the Low Temperature Property of Asphalt fine Aggregate Matrix and Asphalt Mixture Including the Environmental Factors. *Constr. Build. Mater.* 156, 56–62. doi:10.1016/j.conbuildmat.2017.08.142

Han, S., Sun, P., and Fwa, T. F. (2021). Relationships between Internal Structure and Surface Texture of Asphalt Mixtures. *Road Mater. Pavement Des.* 22, 894–909. doi:10.1080/14680629.2019.1691045

Ho, C.-H., and Romero, P. (2011). Using Asphalt Mixture Beams in the Bending Beam Rheometer. *Road Mater. Pavement Des.* 12, 293–314. doi:10.1080/14680629.2011.9695247

Karimi, M. M., Dehaghi, E. A., and Behnood, A. (2021). A Fracture-Based Approach to Characterize Long-Term Performance of Asphalt Mixes under Moisture and Freeze-Thaw Conditions. *Eng. Fracture Mech.* 241, 107418. doi:10.1016/j.engfracmech.2020.107418

Keshavarzi, B., Mocelin, D., and Kim, Y. R. (2021). Predicting Thermal Stress Restrained Specimen Test Fracture Temperatures Using the Dissipated Pseudo Strain Energy Criterion. *J. Transp. Eng. Part. B Pavements* 147, 04020088. doi:10.1061/jpeodx.0000236

Li, L., Huang, Y., Shao, Z., and Ren, D. (2021). An Experimental Investigation on the Repairing Performance and Fatigue Life of Asphalt Pavement Potholes with an Inclined Interface Joint. *Front. Mater.* 7, 597523. doi:10.3389/fmats.2020.597523

Marasteanu, M., Cannone Falchetto, A., Velasquez, R., and Le, J.-L. (2016). On the Representative Volume Element of Asphalt concrete at Low Temperature. *Mech. Time Depend Mater.* 20, 343–366. doi:10.1007/s11043-016-9302-3

Moon, K. H., Marasteanu, M. O., and Turos, M. (2013). Comparison of Thermal Stresses Calculated from Asphalt Binder and Asphalt Mixture Creep Tests. *J. Mater. Civ. Eng.* 25, 1059–1067. doi:10.1061/(asce)mt.1943-5533.0000651

Qian, Z.-d., Liu, Y., Liu, C.-b., and Zheng, D. (2016). Design and Skid Resistance Evaluation of Skeleton-Dense Epoxy Asphalt Mixture for Steel Bridge Deck Pavement. *Constr. Build. Mater.* 114, 851–863. doi:10.1016/j.conbuildmat.2016.03.210

Qian, G., Yang, H., Li, X., Yu, H., Gong, X., and Zhou, H. (2021). A Unified Strength Model of Asphalt Mixture Considering Temperature Effect. *Front. Mater.* 8, 754187. doi:10.3389/fmats.2021.754187

Romero, P., and Masad, E. (2001). Relationship between the Representative Volume Element and Mechanical Properties of Asphalt concrete. *J. Mater. Civ. Eng.* 1, 77–84. doi:10.1061/(asce)0899-1561(2001)13:1(77)

Shan, L., Yang, H., Tian, D., and Tan, Y. (2020). Evaluation of Anti-icing Emulsified Asphalt Binders. *Front. Mater.* 7, 257. doi:10.3389/fmats.2020.00257

Shi, L., Wang, D., Wang, J., Jiang, Z., Liang, H., and Qin, X. (2020). A New Method for Designing Dense Skeleton Asphalt Mixture Based on Meso Parameter. *Adv. Civil Eng.* 2020, 1–13. doi:10.1155/2020/3841291

Thomas, K. P. (2002). Impact of Water during the Laboratory Aging of Asphalt. *Road Mater. Pavement Des.* 3, 299–315. doi:10.1080/14680629.2002.9689927

Underwood, B. S., and Kim, Y. R. (2013). Effect of Volumetric Factors on the Mechanical Behavior of Asphalt fine Aggregate Matrix and the Relationship to Asphalt Mixture Properties. *Constr. Build. Mater.* 49, 672–681. doi:10.1016/j.conbuildmat.2013.08.045

Velásquez, R., Marasteanu, M., Turos, M., and Labuz, J. (2009). "Effect of Beam Size on the Creep Stiffness of Asphalt Mixtures at Low Temperatures," in *Advanced Testing and Characterization of Bituminous Materials, Two Volume Set* (London, United Kingdom: CRC Press), 329–338. doi:10.1201/9780203092989

Wang, Y., Ye, J., Liu, Y., Qiang, X., and Feng, L. (2013). Influence of Freeze-Thaw Cycles on Properties of Asphalt-Modified Epoxy Repair Materials. *Constr. Build. Mater.* 41, 580–585. doi:10.1016/j.conbuildmat.2012.12.056

Wang, F., Xiao, Y., Cui, P., Ma, T., and Kuang, D. (2020). Effect of Aggregate Morphologies and Compaction Methods on the Skeleton Structures in Asphalt Mixtures. *Constr. Build. Mater.* 263, 120220. doi:10.1016/j.conbuildmat.2020.120220

Wang, W., Luo, R., Li, J., and Wang, L. (2022). Evaluation on the Influence of Dynamic Water Pressure Environment on Viscoelastic Mechanical Performance of Asphalt Mixture Using the Bending Beam Rheometer Method. *Constr. Build. Mater.* 321, 126428. doi:10.1016/j.conbuildmat.2022.126428

Weissman, S. L., Harvey, J., Sackman, J. L., and Long, F. (1999). Selection of Laboratory Test Specimen Dimension for Permanent Deformation of Asphalt Concrete Pavements. *Transport. Res. Rec.* 1681, 113–120. doi:10.3141/1681-14

Xing, C., Liang, Z., Tan, Y., Wang, D., and Zhai, C. (2021). Skeleton Filling System Evaluation Method of Asphalt Mixture Based on Compressible Packing Model. *J. Transp. Eng. Part. B Pavements* 147, 04021062. doi:10.1061/jpeodx.0000320

Xu, H., Guo, W., and Tan, Y. (2015). Internal Structure Evolution of Asphalt Mixtures during Freeze-Thaw Cycles. *Mater. Des.* 86, 436–446. doi:10.1016/j.matdes.2015.07.073

Xu, H., Guo, W., and Tan, Y. (2016). Permeability of Asphalt Mixtures Exposed to Freeze-Thaw Cycles. *Cold Regions Sci. Techn.* 123, 99–106. doi:10.1016/j.coldregions.2015.12.001

Yang, S., Jiang, J., Leng, Z., and Ni, F. (2021). Feasibility and Performance of the Semi-circular Bending Test in Evaluating the Low-Temperature Performance of Asphalt Mortar. *Constr. Build. Mater.* 269, 121305. doi:10.1016/j.conbuildmat.2020.121305

Yin, A., Yang, X., Yang, S., and Jiang, W. (2011). Multiscale Fracture Simulation of Three-point Bending Asphalt Mixture Beam Considering Material Heterogeneity. *Eng. Fracture Mech.* 78, 2414–2428. doi:10.1016/j.engfracmech.2011.06.001

Yu, T., Zhang, H., and Wang, Y. (2020). Interaction of Asphalt and Water between Porous Asphalt Pavement Voids with Different Aging Stage and its Significance to Drainage. *Constr. Build. Mater.* 252, 119085. doi:10.1016/j.conbuildmat.2020.119085

Yu, H., Yao, D., Qian, G., Cai, J., Gong, X., and Cheng, L. (2021). Effect of Ultraviolet Aging on Dynamic Mechanical Properties of SBS Modified Asphalt Mortar. *Constr. Build. Mater.* 281, 122328. doi:10.1016/j.conbuildmat.2021.122328

Zhang, Y., and Leng, Z. (2017). Quantification of Bituminous Mortar Ageing and its Application in Ravelling Evaluation of Porous Asphalt Wearing Courses. *Mater. Des.* 119, 1–11. doi:10.1016/j.matdes.2017.01.052

Zhang, X., Zhang, F., Zhou, X., Xu, X., and Chen, X. (2021). Multi-scale Evaluation of the Mechanical Properties of Asphalt Mortar under Different Aging Conditions. *Mol. Simul.* 8, 1–12. doi:10.1080/08927022.2021.1902518

Zhou, J., Chen, X., Xu, G., and Fu, Q. (2019). Evaluation of Low Temperature Performance for SBS/CR Compound Modified Asphalt Binders Based on Fractional Viscoelastic Model. *Constr. Build. Mater.* 214, 326–336. doi:10.1016/j.conbuildmat.2019.04.064

Conflict of Interest: The authors declare that they have no known competing financial interests or personal relationships that could have appeared to influence the work reported in this paper.

Publisher's Note: All claims expressed in this article are solely those of the authors and do not necessarily represent those of their affiliated organizations, or those of the publisher, the editors and the reviewers. Any product that may be evaluated in this article, or claim that may be made by its manufacturer, is not guaranteed or endorsed by the publisher.